8.2 MEASUREMENT OF GROWTH AND DENSITY OF DENDRITE CRYSTALS

John Hallett* and Brett W. Garner
Desert Research Institute, Reno, Nevada USA

SUMMARY

Growing ice particles and mixed phase particles in the atmosphere, such as melting snow or freezing drops, have complex shapes and internal density distributions due to variable environmental conditions encountered during fall. Particle mean density may be expressed as mass spread over an equivalent sphere defined by projected particle extremities, the equivalent for a planar crystal or in terms of an equivalent melted diameter. The variety of particle shapes and sizes present unique problems in characterizing their densities. Different density distributions may be inferred from particle images and measured by particle capture and real time evaporation. Direct measurements of density are made by a cloudscope, an instrument that captures and sublimes particles while video recording from the rear of an optical surface. Measurements made by a high-resolution instrument have uncertainties of ± 0.01 g cm^{-3}. Densities of atmospheric particles are measured from the tropical upper troposphere in both Pacific and Atlantic environments and range from 0.03 to 0.91 g cm^{-3} with an average of 0.41 g cm^{-3}. There is evidence of riming of faceted atmospheric particles through exposure of residual facets following evaporation. Many particles showed variable densities, with a low density outer shell surrounding a higher density inner core; openness of the structure is quantified through the rate of change of the area of ice as it sublimes.

1. INTRODUCTION

Atmospheric particles come in a variety of shapes and sizes, from the regular geometrical shapes defined by lattice growth, to irregular shapes produced through aggregation and riming. It is insufficient to assume these particles have a density in the proximity of solid ice (0.92 g cm^{-3} to sufficient accuracy) or even a constant density. Consider a faceted ice crystal with a high degree of geometrical symmetry. As the crystal moves through the atmosphere encountering different environmental conditions, it may become hollow, grow dendritic arms, or rime and aggregate with other particles. The *local* density of atmospheric particles is specified as the mass of an incrementally small sphere or cylinder of size such that uniformity may be assumed and ignoring any uncertainties arising from the statistics of molecular processes of growth or sublimation. In practice, water drops have a density influenced by solute concentration and temperature; ice particles have a density influenced by the presence of air, either as inclusions or as bubbles formed by rejection of air from solution during solidification.

Atmospheric processes result in a wide range of possible particle densities. The lowest extreme density can be defined by the geometrical distribution of mass such as a frozen spherical shell or bubble having a mean density less than 0.001 g cm^{-3}, while at the other extreme solid ice is formed when air is excluded by slow freezing of a droplet spreading on impact on an ice surface or by growth of a solid faceted crystal from the vapor. Some geometries intrinsically exhibit low density such as a bullet rosette or dendrite with a six fold array, Fig. 1. In reality, the actual densities of particles are dispersed between these two extremes. For example, a conical graupel particle grows by accretion of droplets at its base as it falls in a fixed orientation, so that the apex, possibly beginning as a 0.92 g cm^{-3} density frozen drop, becomes “fluffy” by frost growth from the vapor or low density droplet accretion and increases in density again toward the bottom as its fall velocity increases and the growth conditions change.

Particle density is required to calculate many atmospheric quantities. A particle falling at terminal velocity has an associated drag

*Corresponding author address: Dr. John Hallett, Division of Atmospheric Sciences, Desert Research Institute, 2215 Raggio Parkway, Reno, NV 89512-1095. E-mail: John.Hallett@dri.edu

force due to a difference in velocity between the particle and the fluid and is dependent through a drag coefficient on the fluid properties as well as the shape and density of the falling particle. Once the terminal velocity and particle mass are known, other quantities may be calculated, such as the mixing ratio and precipitation rates. The vertical mass flux (measured relative to updrafts and downdrafts), important for aircraft where supercooled water can freeze on aircraft wings causing loss of aerodynamic lift, also can be calculated (Hallett and Isaac 2002, 2009). Understanding the density of particles also plays a key role in characterizing electromagnetic wave interactions, within the atmosphere, as realized in 1871 by Lord Rayleigh (Strutt 1871) as he studied the relationship between particles and refraction in the atmosphere. Electromagnetic interactions, particularly in the radar portion of the spectrum, are critical as a tool in understanding atmospheric processes (Um and McFarquhar 2007). The optical properties of any cloud are a function, among other things, of the concentration of particles and their density. In general, electromagnetic radiation interacts more strongly with solid particles than with low density particles (McFarquhar et al. 2002; Yang et al. 2008).

We address the question of the density of a particle, as having a volume of a sphere for three dimensional (3D) examples and a cylinder for two dimensional (2D) examples, defined by points on an outer periphery. Further, direct measurement of densities has been obtained from the cloudscope, an instrument that collects particles on a heated optical flat mounted normal to the airstream, the rate of change of particle area through sublimation being inversely related to density (Hallett et al. 1998; Meyers and Hallett 2001; Vidaurre and Hallett 2009). Particles fall conveniently into two categories; those with a uniform density and those showing significantly different densities at various locations.

2. DEFINITION OF DENSITY

Complex, non-symmetrical crystals such as rimed or aggregate particles create difficulty in defining density. One solution is to use an increasingly complex bounding volume to describe the crystal.

Empirical power series with two variables may approximate density as $\rho = aD^n$ (see for example, Arnott et al. 1994). An obvious problem with such relationships is the ambiguity in classifying crystal type, and defining D from an arbitrary point where a stellar crystal changes from narrow arms to broad arms. In addition, crystals will have encountered unique environmental conditions (temperature, supersaturation, droplet accretion, and size) resulting in different growth geometries and giving a wide spread of values of the coefficients a and n, significantly reducing the utility of this relationship.

In practice, the density of a particle may be found by many different techniques, requiring a measurement of particle dimension with an estimation of mass or applying the dimensions to a relationship developed from non-related data. Alternatively, a definition may be made from an optical viewpoint, relating the mass of a sphere to a projected area to serve as a convenient measure of optical transfer path and provides a measure of equivalent diameter in terms of ice-water content (Stephens 1990; Mitchell 2002). This assumes a uniformity of ice density, as will be shown to be only justified in special cases, as opposed to an expected uniformity of water density for liquid drops when the size spectrum alone is sufficient. These considerations apply either in one dimension (1D) as in the growth of a column, needle, linear crystal or rime (Dong and Hallett 1989), in 2D as in the growth of a flat dendrite or in 3D as in the growth of a spatial dendrite or bullet rosette. The mean density of the particle depends on an assumed outer geometry as a simple cylinder or sphere. In practice, the *local* density of the particle depends on the location related to the site and direction of growth and must be assigned a convenient reference, such as a centroid with 6 fold or other symmetry to be averaged over a series of narrow annuli or thin shells for the entire particle.

2.1. *Effective diameter*

First studies of geometries of ice crystals in the atmosphere began applying descriptors such as shape, thickness and diameter (see for example Ono 1969; Auer 1970). Ice crystals exhibiting a basic cylindrical shape – such as columns, bullets and needles – are

approximated using a cylindrical volume (Platt 1997). There are two categories for defining equivalent diameter (Wyser 1998; McFarquhar and Heymsfield 1998) with the simplest equivalent diameter being parameterized using liquid water content (Boudala et al. 2002). The ice content may be derived from spectra of images of particle shapes and temperature, but requires a density to be specified completely.

The effective diameter, for spherical particles such as liquid water droplets, can be defined uniquely where both the ratio of volume to projected area and the mean scattering particle cross section are identical. The simplest definition is where the ratio of volume-to-projected area and the mean cross section are equivalent (Han et al. 1998). Other systems define only an equivalent volume or cross section for a sphere (Ebert and Curry 1992; McFarquhar and Heymsfield 1996; McFarquhar and Black 2004; Rolland et al. 2000). For non-spherical particles such as dendrites, aggregate and rimed particles, these two quantities cannot be identical because of variations in the cross section and the concept of effective diameter completely breaks down, lacking physical reality.

2.2. Density of two dimensional crystals

It is clear that neither highly symmetric crystals nor irregular particles have a constant density throughout their structure. Gaps greatly reduce the density of a particle from that of the material ice. For example, flat dendrites as discussed herein do not have a constant density throughout the crystal but change with location depending on the growth history. Figures 1 through 5 (crystals from Bentley and Humphreys 1962) depict an area proportional to a planar density annulus plotted against radial distance. The planar areas are found by subdividing the crystal images into annuli counting pixels that contained ice, and scaling the pixel areas. The area of these plots provides a measure of openness of the structure.

The simplest configuration (Fig. 1) depicts a dendrite with narrow arms extending from a well defined center and a decreasing density due to the increase in spacing between the arms toward the periphery. The solid dendrite center represents a density approaching ice, 0.92 g cm^{-3} and is shown as point A (Fig. 2). This also depicts a more complex dendrite with plate growth (Hallett and Mason 1958; Keller and Hallett 1982; Bailey and Hallett 2009) on the arms with more complex shapes and density variation outward (Figs. 3, 4, and 5).

The local area is assumed to be zero density (black) or normalized to 1 (white, as solid crystal), the crystal having uniform thickness in the direction of viewing. Dendrites viewed edge on verify such an assumption to sufficient accuracy. The central regions of all hexagonal crystals are usually a simple solid ice hexagonal prism. Moving outward along a radius from the center, a varying amount of ice area is encountered beyond the hexagon until it vanishes at r = Rmax. Depending on the growth history of the crystal, the local density decreases monotonically (Fig. 3) or alternates (Fig. 2). Since the density is defined as the local area of crystal related to the area of an ice disk extending to the periphery, the mean density (as the area of the plots) represents the openness of the structure. Thus, the radial variation of the distribution of ice density is related to the observed area evaporation rate $\frac{dA}{dt}$, as a measure of the local ice density, (determined by its original conditions of growth from the vapor, Appendix, Equation 6). A comparable analysis is applicable to an evaporating column (possibly hollow) viewed from its top or side. The graphs were constructed by measurement of the area at the intersection of each crystal part with annuli centered in the hexagon. It is clear that the hexagonal crystal arms and side branches often are not quite symmetrical, resulting from irregularities during growth, adding further to the complexity.

3. AIRCRAFT MEASUREMENT OF ICE PARTICLE DENSITY

Measurement of the density of atmospheric ice particles makes use of the cloudscope. This instrument incorporates a forward facing optical flat maintained at the dynamic temperature, upon which particles impact and are video recorded. The result is the ability to measure the density of atmospheric ice particles by way of sublimation and/or melting of the particle

(Hallett et al. 1998; Hallett and Isaac 2009). Data (Table 1) are taken from NASA DC8 (Fig. 10) in the Kwajalein project (Kingsmill 2004; Garner 2001).

A substance undergoing a phase change, (sublimation in the present case) absorbs latent heat, provided by conduction from the much larger optical flat of the instrument. The temperature on the surface of the ice particle is assumed to be the dynamic temperature at the stagnation point on the optical flat of the cloudscope, sufficiently close to the temperature rapidly reached by any impacted ice particle of much smaller size. In practice, it may be necessary to heat the surface above its stagnation temperature (measured directly by a sensing element in the window) to increase sublimation rate and prevent complete icing of the optics leading to an increased temperature and ice vapor pressure.

The convenient representative volume for rimed particles (or aggregates) is taken as a hemisphere, as an impacting particle must collapse to some extent on impact as the images show. The particle density now relates to T_∞, the ambient temperature, T_s the (measured) surface temperature and $\frac{dA}{dt}$, the measured slope of the of the change in projected area with evaporation and L_s (T_s) the latent heat of sublimation. These quantities are found from the using flight data and and imaging software. Some particles gave evidence of unchanging density during evaporation, as the constant slope (Fig 9) for the particle on Fig 8. A fifth of the particles measured showed at least two densities dependent on radius, interpreted as a particle with a fluffy low density exterior and a high density interior (Fig 6,7). The inference of several densities in the analysis as distinct areas under the sublimation curves is not artifact as the density curve has a sharp discontinuity, not expected as a variable impact collapse. Further, the dense inner core is revealed as the outer surface of the particle sublimes. Fig 12 shows that the same process takes place for a lightly rimed particle, suggesting that the particles first formed and then fell through a volume of supercooled droplets freezing as they contacted the core particle. Rime formed on a particle can be denser, near solid ice if the temperature is near 0°C or less dense at lower temperature and growth rate. Given that KWAJEX data were taken at temperatures between -35°C and -60°C, lower density rime is only expected at temperatures above -40°C, the expected limit of supercooled water and the ability to have a low density. It is of interest that of the 255 particles analyzed no residual nuclei (> 1 μm) remained after evaporation, implying a lack of such nuclei when the ice particles formed or were collected subsequently by scavenging.

4. CONCLUSIONS

The range and spread of density of an ice particle influence estimates of mass, fall velocity and orientation, evaporation and melting breakup and electromagnetic properties over a wide range of wavelengths. The definition of density of any ice particle, may conveniently follow a conceptual approach from an observed shape or a measurement protocol through sublimation, assuming a mix of ice and air spaces with zero density. In addition, the following need consideration:

- The likelihood of an internal mix of water and ice (spongy growth) as an enhancement of density above that of ice alone (0.92 compared with water 1.0).

- Rejection on freezing of significant denser solutes (as from sea water) and clathrates may complicate matters.

- Interpretation of spatial distribution and shape of air spaces provides a historical growth record to constrain environmental conditions, as Temperature, Super-saturation, Fall Velocity, Air Pressure. The changing area of the spaces provide a quantitative measure of structure openness.

- There remains a great mystery leading to trigonal symmetry of a central hexagonal ice particle (about one in ten crystals in Bentley & Humphries 1962; Hallett et al. 2002; and also Scoresby 1820 Fig. 11).The presence of stacking faults is not an uncommon feature of ice growth.

Densities in the measurements ranged from 0.03 g cm^{-3} up to 0.92 g cm^{-3}, with an average of 0.41 ±0.22 g cm^{-3} and an uncertainty for particle diameter of 1 μm. A wide variety of particle shapes were found such as columns, rimed columns, bullet rosettes, needle (extreme 'c' axis growth), and graupel particles resulting from supercooled drop accretion.

This data illustrates that the potential exists for a wide spread of particle density, knowledge necessary for characterization of atmospheric processes involving the ice phase; any model needs to take this into account. As a research tool, cloudscope analysis provides direct measurement of particle habit and density.

5. ACKNOWLEDGEMENT

The work in the thesis was funded by grants from: NASA FIRE III (NAG-1-2046), NASA In-Situ TRMM/KWAJEX (NAG-5-7973), NSF Ice Growth (ATM-9900560), NSF SGER (ATM-0003192), NASA TRMM / KWAJEX OBS (NAG-5-9716).

6. REFERENCES

Arnott, W.P., Y.-Y Dong, J. Hallett, and M.R. Poellot, 1994: Role of small ice crystals in radiative properties of cirrus: A case study, FIRE II, November 22, 1991. *J. Geophys. Res.,* **99**(D1)**,** 1371-1381.

Auer, A.H., D.L. Veal, 1970: The Dimension of Ice Crystals in Natural Clouds, *J. Atmos. Sci*., **11**, 919-926.

Bailey, M.P., and J. Hallett, 2009: A Comprehensive Habit Diagram for Atmospheric Ice Crystals: Confirmation from the Laboratory, AIRS II, and Other Field Studies. *J. Atmos. Sci.*, **66**, 2888-2899. doi: 10.1175/2009JAS2883.1.

Bentley, W.A. and W.J. Humphreys, 1962: *Snow Crystals*. New York: Dover Publications.

Boudala, F.S., G.A. Isaac, W. Fu, and S.G. Cober, 2002: Parameterization of Effective Ice Particle Size for High Latitude Clouds, *Int. J. Climatol*, **22**, 1267-1284.

Dong, Y.Y., and J. Hallett, 1989: Droplet accretion during rime growth and the formation of secondary ice crystals, *Q. J. Roy. Soc.*, **115**, 127-142.

Ebert, E.E. and J.A. Curry 1992: A Parameterization of Ice Cloud Optical Properties for Climate Models, *J. Geophys. Res.* **97**, 3831-3836.

Garner, B., 2001: On the Density of Atmospheric Particles. Thesis, Master of Science, University of Nevada, Reno.

Hallett, J., W.P. Arnott, M.P. Bailey, and J.T. Hallett, 2002: Ice Crystals in Cirrus, in *Cirrus*, edited by K.D. Lynch, K. Sassen, D. O'C. Starr, G. Stephens, Chpt. 3, pp. 41-77, Oxford University Press, Inc., New York.

Hallett, J. and G. Isaac, 2002. Aircraft Icing in Glaciated and Mixed Phased Clouds. *40th AIAA Aerospace Meeting and Exhibit*, AIAA 2002-0677, Reno, NV.

Hallett, J., W.P. Arnott, R. Purcell and C. Schmidt, 1998: A Technique for characterizing Aerosol and Cloud Particles by Real Time Processing. *$PM_{2.5}$: A fine particle standard Proceedings of an International Specialty Conference,* Sponsored by *EPA Air & Waste Management Association,* Ed. By J. Chow and P. Koutrakis, 1998, **1**, 318-325.

Hallett, J. and G.A. Isaac, 2009: Aircraft Icing in Glaciated and Mixed Phase Clouds. *J. Aircraft,* **45**(6), 2120-2130.

Hallett, J., and B.J. Mason, 1958: The influence of temperature and supersaturation on the habit of ice crystals grown from the vapour, *Proc. Roy. Soc*., **A247**, 440-453.

Han, Q., W.B. Rossow, J. Chou, and R.M. Welch, 1998: Global Survey of the Relationships of Cloud Albedo and Liquid Water Path with Droplet Size Using ISCCP, *J. Climate*, **11**, 1516-1528.

Heymsfield, A.J., A. Bansemer, and C.H. Twohy, 2007: Refinements to Ice Particle Mass Dimensional and Terminal Velocity Relationships for Ice Clouds. Part I: Temperature Dependence. *J. Atmos. Sci.,* **64,** 1047-1067.

Keller, V. and J. Hallett, 1982: Influence of air velocity on the habit of ice crystal growth from the vapor, *J. Crystal Growth*, **60**, 91-106.

Kingsmill, D., S. Yetter, A. Heymsfield, P. Hobbs, A. Korolev, J. Stith, A. Bansemer, J. Haggerty, and A. Rangno, 2004: TRMM Common Microphysics Products: A tool for Evaluating Spaceborne Precipitation Retrieval Algorithms. *J. Appl. Meteor*., **43**, 1598-1618.

McFarquhar, G.M., and R.A. Black, 2004: Observations of Particle Size and Phase in Tropical Cyclones: Implications for Mesoscale Modeling of Microphysical Processes. *J. Atmos. Sci.,* **61,** 442-439.

McFarquhar, G.M. and A.J. Heymsfield, 1996: Microphysical Characteristics of Three Anvils Sampled during the Central Equatorial Pacific Experiment, *J. Atmos. Sci*., **53**, 2401-2423.

McFarquhar, G.M. and A.J. Heymsfield, 1998: The Definition and Significance of an Effective Radius for Ice Clouds, *J. Atmos. Sci*., **55**, 2039-2052.

McFarquhar, G.M., P. Yang, A. Macke, and A. J. Baran, 2002: A new parameterization of single-scattering solar radiative properties for tropical anvils using observed ice crystal size and shape distributions. *J. Atmos. Sci.,* **59,** 2458-2478.

Meyers, M.B. and J. Hallett, 2001: Micrometer-sized hygroscopic particles in the atmosphere: Aircraft measurement in the Arctic. *J. Geophys. Res*, **106 (D24)**, 34,067-34,080.

Mitchell, D.L., 2002: Effective Diameter in Radiation Transfer: General Definition, Applications, and Limitations, *J. Atmos. Sci.*, **59**, 2330-2346.

Ono, A., 1969: The shape and riming properties of ice crystals in natural clouds, *J. Atmos. Sci.*, **26**, 138-147.

Platt, A.M.R., 1997: A Parameterization of the Visible Extinction Coefficient of Ice Clouds in Terms of the Ice/Water Content, *J. Atmos. Sci.*, **54**, 2083-2098.

Rolland, P., K.N. Liou, M.D. King, S.C. Tsay, and G. M. McFarquhar, 2000: Remote sensing of optical and microphysical properties of cirrus clouds using Moderate-Resolution Imaging Spectroradiometer channels: Methodology and sensitivity to physical assumptions, *J. Geo. Res.*, **105**, 11721-11738.Boston: Kluwer Academic Publishers.

Ryan, B.F., E.R. Wishart, and D.E. Shaw, 1976. The Growth Rates and Densities of Ice Crystals between -3°C and -21°C. *J. Atmos. Science*, **33**, 842-850.

Scoresby, W., 1820: *An account of the Arctic regions with a history and description of the northern whale fishery*. Vol. I, p. 551. Archibald Constable and Co., Edinburgh.

Stephens, G.L., S.C. Tsay, P.W. Stackhouse, and P. J. Flatau, 1990: The relevance of the microphysical and radiative properties of cirrus clouds to climate and climatic feedback. *J. Atmos. Sci.,* **47,** 1742-1753.

Strutt, J. (Lord Rayleigh), 1871. On the Light from the Sky, Its Polarization and Color, *Phil. Mag.* **41**, 107-120.

Um, J., and G.M. McFarquhar, 2007: Single-Scattering Properties of Aggregates of Bullet Rosettes in Cirrus. *J. Appl. Met. Clim.,* **46,** 757-775**.**

Vidaurre, G., and J. Hallett: 2009: Particle Impact and Breakup in Aircraft Measurement. *J. Atmos. & Oceanic Technol*. **26**(5), 972-983.

Wyser, K., 1998: The Effective Radius in Ice Clouds, *J. Climate*, **11**, 1793-1802.

Yang, P., Z. Zhang, G.W. Kattawar, S.G. Warren, B.A. Baum, H.-L. Huang, Y.X. Hu, D. Winker, and J. Iaquinta, 2008: Effect of Cavities on the Optical Properties of Bullet Rosettes: Implications for Active and Passive Remote Sensing of Ice Cloud Properties, *J. J. Appl. Met. Clim.,* **47,** 2311-2329.

APPENDIX

Using the analogy between the vapor field around a particle and the electrostatic potential around a charged conductor of the same geometry and size, the rate of change in mass m is given by

$$\frac{dm}{dt} = 2\pi r D(\rho_\infty - \rho_s) \quad (1)$$

where D is the diffusion coefficient of water in the air, ρ_∞ the ambient vapor density, and ρ_s is the vapor density at the surface of the particle, approximated by the sapphire window temperature.

The rate of heat loss may be written in terms of the thermal conductivity of air (k)

$$\frac{dQ}{dt} = 2\pi r k(T_s - T_\infty) \quad (2)$$

where T_∞ is the aircraft measurement of ambient temperature and T_s is measured directly by a sensor imbedded in the window.

The closest representative volume for most aggregates and rimed particles is that of a sphere. When a particle impacts on the window of the cloudscope one side collapses resulting in a hemisphere. Therefore, with the assumption of spherical symmetry yielding the mass for a hemisphere:

$$m = \frac{2}{3}\pi r^3 \rho_p \quad (3)$$

It is assumed that the ice density is constant ρ_p over the time dt. Since in practice the density of particles is dependent upon the radius, we need only to choose a small enough time interval justifying the density to be constant. Thus, the rate of change in the mass of the hemisphere

$$\frac{dm}{dt} = 2\rho_p \pi r^2 \frac{dr}{dt} \quad (4)$$

The projected area of a hemisphere on the window is $A = \pi r^2$. The rate of change of the area is

$$\frac{dA}{dt} = 2\pi r \frac{dr}{dt} \quad (5)$$

giving

$$\rho_p = \frac{2\pi k(T_\infty - T_s)}{L_s(T_s)} \frac{1}{\frac{dA}{dt}} \quad (6)$$

where $\frac{dA}{dt}$ is obtained directly from the imaging software for each particle from impaction until complete evaporation.

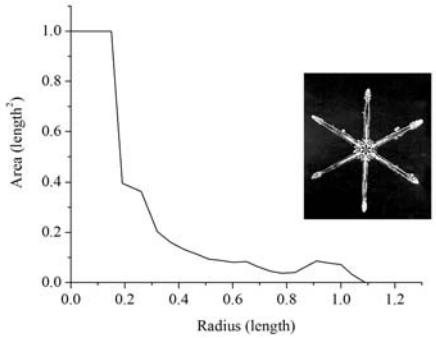

FIG. 1. Radius dependent of ice area on a stellar crystal with narrow arms and a solid plate center. The effective area of ice falls rapidly with radius from the inner plate and increases slightly with additional growth near the crystal tips.

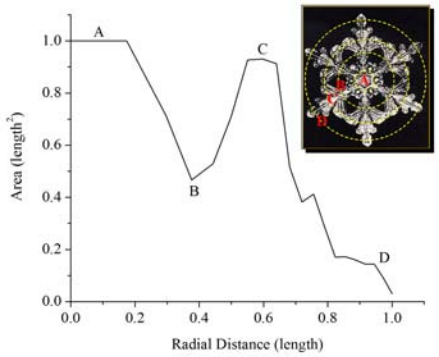

FIG. 2. Plot similar to Fig. 1, shows a plate interior of constant density (A); a deficit of ice between side arms (B); extensive side arm grown (C); a bounding circle through newly grown dendrite tips (D).

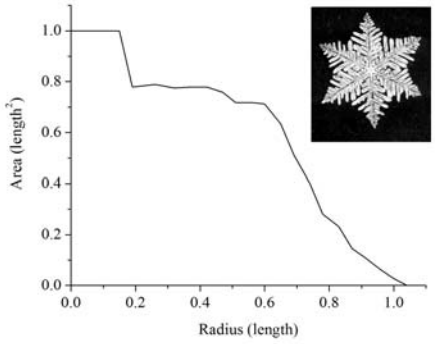

FIG. 3. A highly branched closely spaced arm dendrite showing high density until half way out beyond which freshly grown dendrite branches result in density falling to low values.

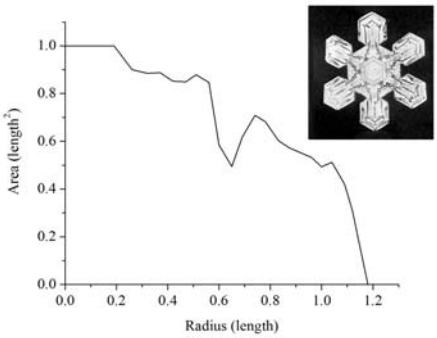

FIG. 4. Large plate surrounded by sector plates showing more uniform ice area coverage.

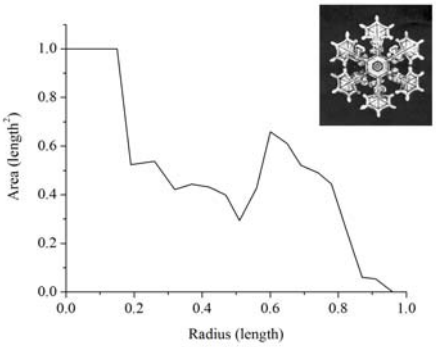

FIG. 5. Similar to Fig. 4 with distinct gaps between outer plates each with a narrow tip growth.

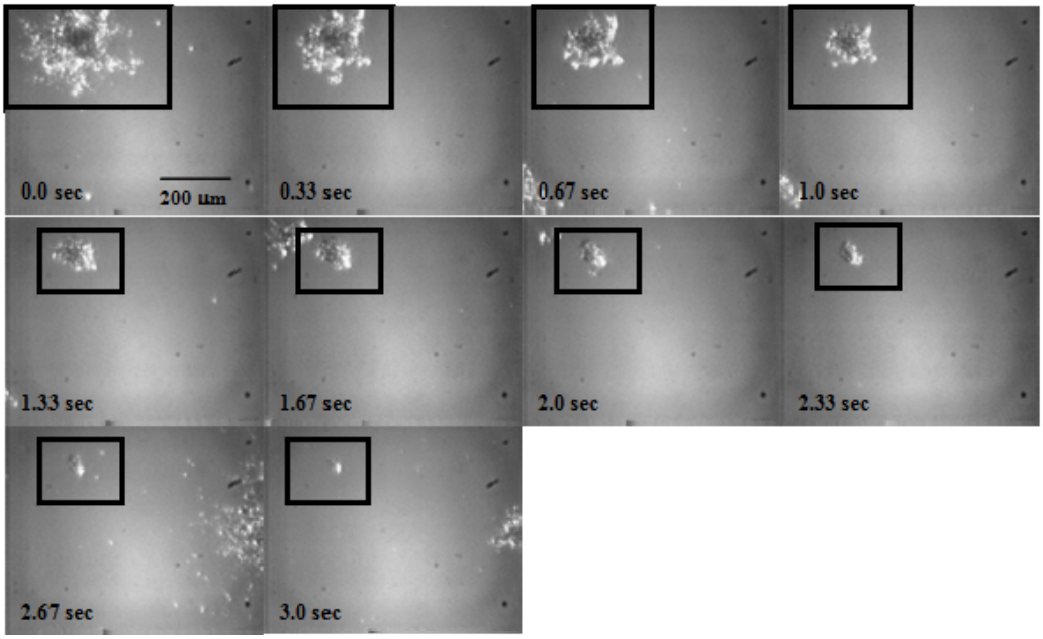

FIG. 6. A particle with two different densities computed from Equation 6 (Appendix), a fluffy outer shell and a solid inner sphere,

the density as $\frac{dA}{dt}$ is obtained directly from the imaging software for each particle from impaction until complete sublimation.

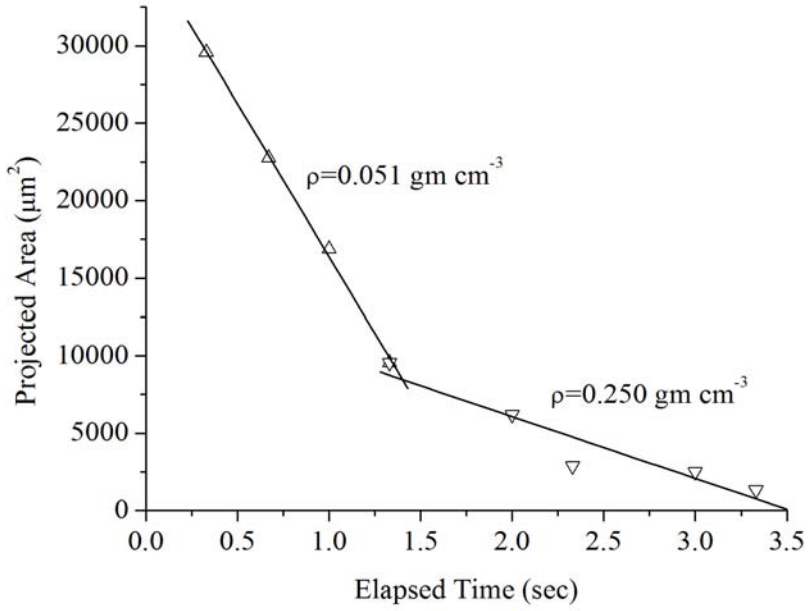

FIG. 7. Sublimating particle shown in Fig. 6 with an outer low density and a higher density core.

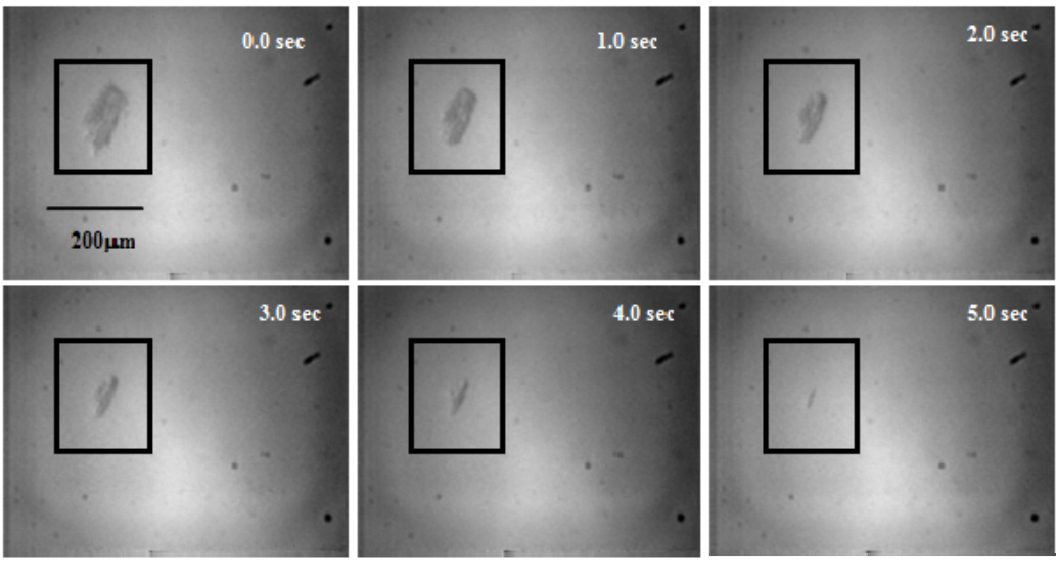

FIG.8. A sublimating particle with a uniform density.

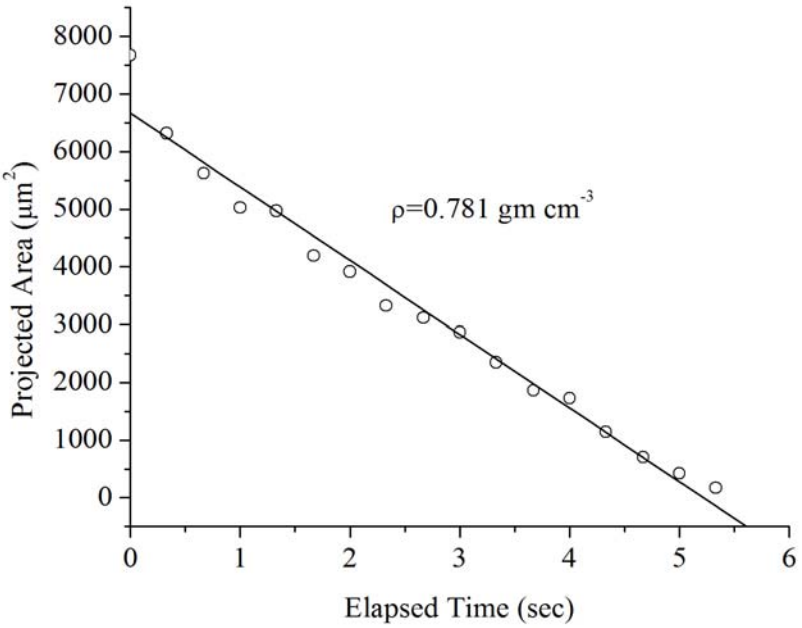

FIG. 9. Sublimating particle from Fig. 8 showing a uniform density.

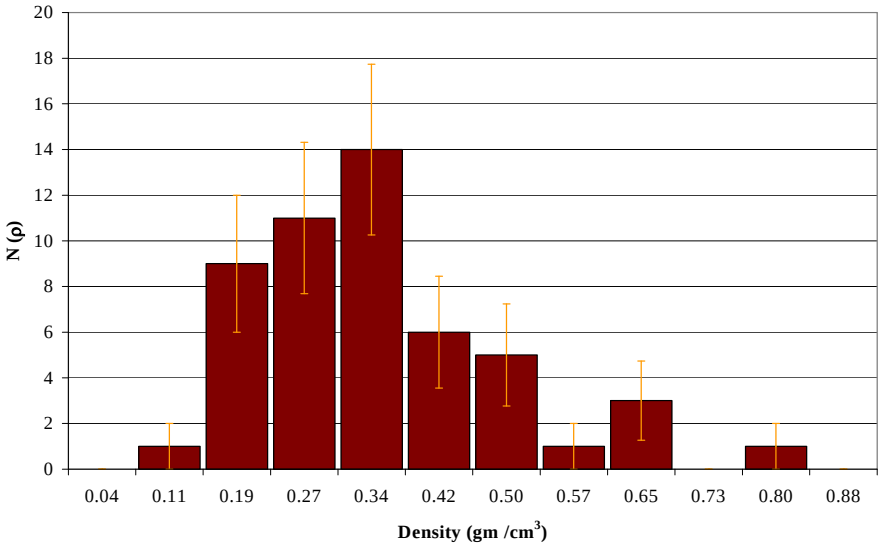

FIG. 10. CAMEX density distribution of time segments 10:59:51 to 11:00:00 (NASA DC8) 980414.

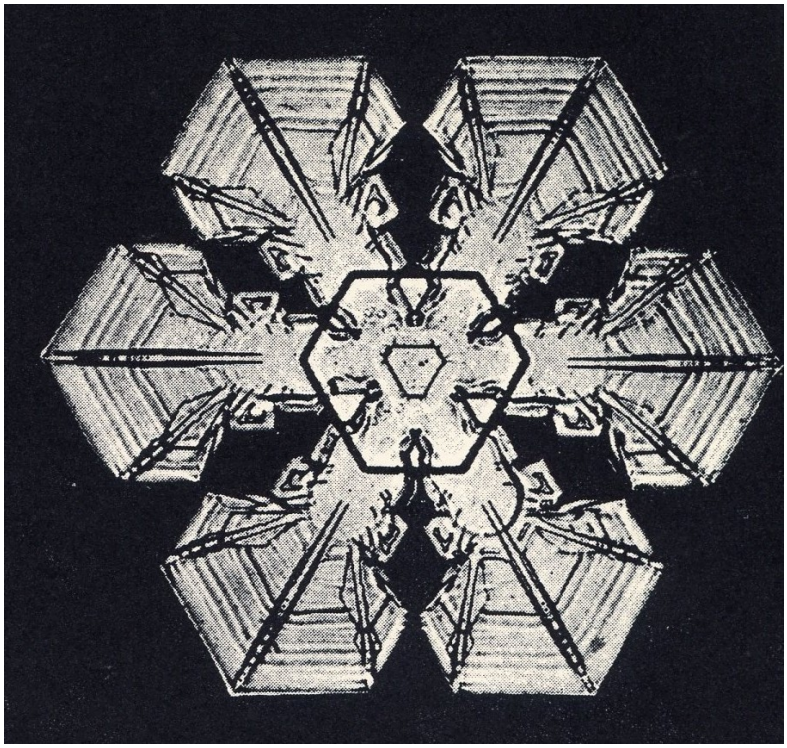

FIG. 11. Central trigonal symmetry of a hexagonal crystal.

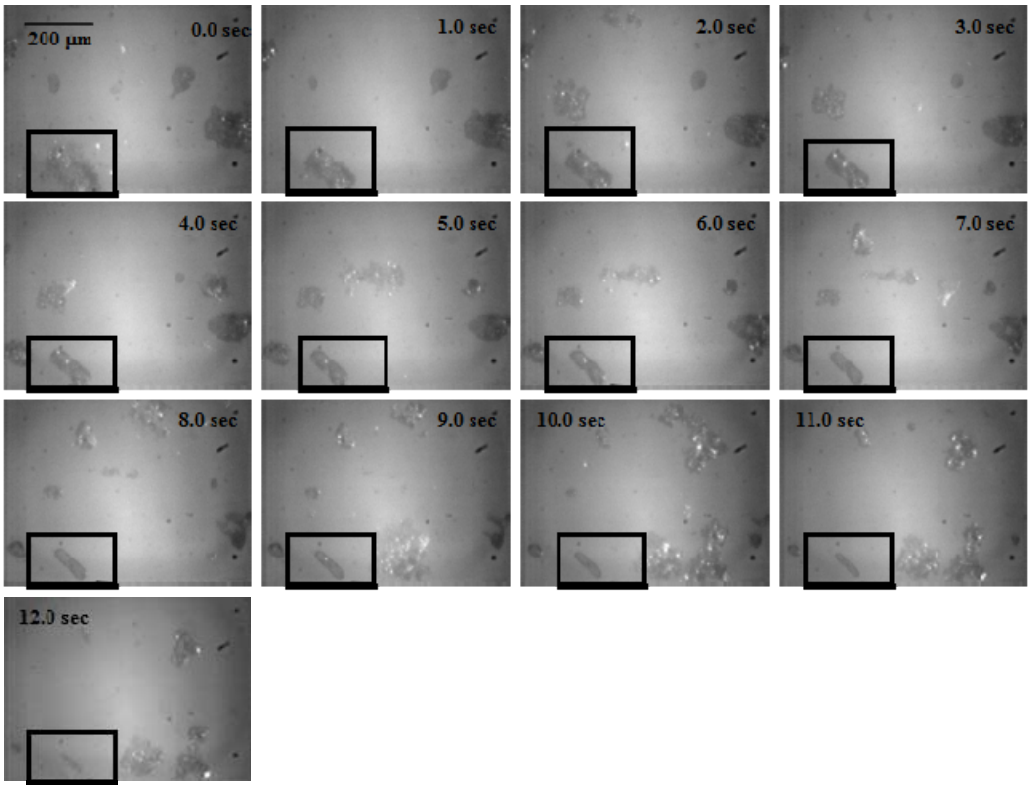

FIG. 12. A rimed column, with rime sublimating first before leaving the inner column.

Initial Time	Elapsed Time	Average Density	Standard Deviation	Density High Volume	Density Low Volume	Number of Particles
KWAJEX						
3:07:55	1 hr 20 min	0.340	0.247	0.911	0.060	47
4:42:22	1 hr 35 min	0.208	0.113	0.500	0.033	52
3:48:08	1 hr 10 min	0.553	0.210	0.910	0.056	60
5:27:15	52 min	0.325	0.199	0.718	0.105	11
10:38:02	1 hr 32 min	0.456	0.273	0.913	0.110	63
21:22:24	-------	0.170	-------	------	------	1
22:30:57	1 hr 42 min	0.351	0.193	0.673	0.181	9
00:40:22	47 min	0.632	0.152	0.878	0.357	14
3:45:17*	1 min	0.450	0.199	0.881	0.106	98

Table 1. A summary of the KWAJEX particle densities. * Denotes the data collected with a large format cloudscope window diameter 3 cm; other data from standard cloudscope diameter 3 mm.